





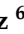

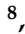

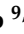

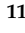



Article

A Multiple-Choice Maze-like Spatial Navigation Task for Humans Implemented in a Real-Space, Multipurpose Circular Arena

Pablo Muela ^{1,2} , Elisa Cintado ^{1,2} , Patricia Tezanos ^{1,2} , Benjamín Fernández-García ^{3,4} , Cristina Tomás-Zapico ^{4,5} , Eduardo Iglesias-Gutiérrez ^{4,5} , Angel Enrique Díaz Martínez ⁶ , Ray G. Butler ⁷ , Victor Cuadrado-Peñañiel ⁸ , Ricardo De la Vega ⁸ , Vanesa Soto-León ⁹ , Antonio Oliviero ^{9,10} , Laura López-Mascarque ¹¹  and José Luis Trejo ^{1,*} 

- ¹ Department Translational Neuroscience, Cajal Institute, CSIC, 28002 Madrid, Spain
 - ² PhD Program in Neuroscience, Autónoma de Madrid University-Cajal Institute, 28002 Madrid, Spain
 - ³ Department Morphology and Cell Biology, Anatomy Area, University of Oviedo, 33006 Asturias, Spain
 - ⁴ Health Research Institute of Asturias (ISPA), 33011 Asturias, Spain
 - ⁵ Department Functional Biology, Physiology Area, University of Oviedo, 33006 Asturias, Spain
 - ⁶ Clinical Laboratory Unit, Department of Sport and Health, Spanish Commission for the Fight against Doping in Sport (Comisión Española para la Lucha Antidopaje en el Deporte—CELAD), 28040 Madrid, Spain
 - ⁷ Butler Scientifics, 08023 Barcelona, Spain
 - ⁸ Department Physical Education, Sport and Human Movement, Universidad Autónoma of Madrid, 28049 Madrid, Spain
 - ⁹ FENNSI Group, Hospital Nacional de Paraplégicos, SESCAM, 45004 Toledo, Spain
 - ¹⁰ Unidad Avanzada de Neurorehabilitación, Hospital Los Madroños, 28690 Brunete, Spain
 - ¹¹ Department of Cellular, Molecular, and Developmental Neurobiology, Cajal Institute, CSIC, 28002 Madrid, Spain
- * Correspondence: jltrejo@cajal.csic.es



Citation: Muela, P.; Cintado, E.; Tezanos, P.; Fernández-García, B.; Tomás-Zapico, C.; Iglesias-Gutiérrez, E.; Díaz Martínez, A.E.; Butler, R.G.; Cuadrado-Peñañiel, V.; De la Vega, R.; et al. A Multiple-Choice Maze-like Spatial Navigation Task for Humans Implemented in a Real-Space, Multipurpose Circular Arena. *Appl. Sci.* **2022**, *12*, 9707. <https://doi.org/10.3390/app12199707>

Academic Editor: Alexander E. Hramov

Received: 2 August 2022

Accepted: 23 September 2022

Published: 27 September 2022

Publisher's Note: MDPI stays neutral with regard to jurisdictional claims in published maps and institutional affiliations.



Copyright: © 2022 by the authors. Licensee MDPI, Basel, Switzerland. This article is an open access article distributed under the terms and conditions of the Creative Commons Attribution (CC BY) license (<https://creativecommons.org/licenses/by/4.0/>).

Abstract: Spatial navigation is a key aspect of human behavior and it is still not completely understood. A number of experimental approaches exist, although most of the published data in the last decades have relied on virtual maze on-screen simulation or not-completely freely moving 3D devices. Some interesting recent developments, such as circular mazes, have contributed to analyze critical aspects of freely moving human spatial navigation in real space, although dedicated protocols only allow for simple approaches. Here, we have developed both specifically designed and home-assembled hardware equipment, and a customized protocol for spatial navigation evaluation in freely moving humans in a real space circular arena. The spatial navigation protocol poses an imitation of a real-space multiple-choice path maze with cul-de-sac and instances of non-linear movement. We have compared the results of this system to those of a number of validated, both virtual and real, spatial navigation tests in a group of participants. The system composed by hardware, the test protocol, and dedicated measure analysis designed in our laboratory allows us to evaluate human spatial navigation in a complex maze with a small and portable structure, yielding a highly flexible, adaptable, and versatile access to information about the subjects' spatial navigation abilities.

Keywords: spatial orientation; virtual navigation; real-space physical navigation; circular maze; maze-type protocol

1. Introduction

Human spatial navigation has been experimentally addressed for decades (for a collection and recent review see for example [1,2]), due to its central role in human behavior and its relevant position for several interconnected tasks [3–6]. Consequently, differences have been reported for healthy adults, children, and elders, as well as affected by different diseases and both in healthy and pathological aging, especially because of neurodegeneration [1,7–12].

Relevantly, spatial navigation is impaired in pathologies such as Alzheimer's disease with intriguing differences in the response to different treatments [13–17]. Investigation in the field of spatial navigation has greatly grown thanks to the work with laboratory rodents and a battery of dedicated protocols devoted to analyzing this brain function [18–20]. To evaluate human spatial navigation, several specific tests have been developed [1,21] as well as tests such as the hidden goal test, directly derived from those used in rodents such as the Morris water maze [22–24]. Recently, a number of tests based on virtual reality and treadmills have appeared, as a means of including into the analysis vestibular, proprioceptive and somatosensory cues (revised by Ekstrom et al. 2018 [1]). However, the relative limitation to free movement is still a challenge [25–27]. To solve this problem, circular mazes for humans have been developed [28] allowing us to compare interventions and therapies both in laboratory rodents and humans, by using tests relying on the same conceptual features, as is the case for the hidden goal test and the one presented here.

The main concerns for the existing mazes and protocols, either virtual or real-space, are the limitations of movement (subjects must be quiet in front of a computer screen, or are tied to a treadmill), potential dizziness of VR systems, the limited space into the laboratories to implement large mazes, the limited use of some maze designs (usually not available for multi-test), the short capacity to adjust difficulty of the test, or the implementation into rooms (not transferable or portable to another location).

For all these reasons, we have tried here to develop a system addressing the reported disadvantages of the available tests. We have built a new system composed of a multi-test circular arena and a novel protocol simulating a complex maze. To compare and validate our system, we have evaluated a highly heterogeneous group of participants in a variety of validated tests covering both path integration and hidden goal test in virtual and real-space settings.

2. Materials and Methods

2.1. Subjects

A total number of 24 healthy people participated in this study. Subjects were recruited from the active staff of the Institute Cajal during 2021. A call was launched by email. Every person that voluntarily responded to the call was selected. Sex, age, and exercise level was considered to select the participants in order to balance as much as possible the number of men and women for sex, the number of people <25, between 26 and 40, and >40 years old for age, and the number of sedentary (<3 h active physical exercise per week) and exercised (≥ 3) for exercise level. Sex, age, and exercise level were self-reported.

All the participants signed an informed consent after the experimental procedure was submitted and approved by the CSIC Ethics Committee (Subcommittee of Ethics) of the Spanish Research Council. This procedure included a "participant information sheet" and a "Informed Consent Page" to sign.

The inclusion criteria were: age over 18 years, to be hired for the Institute Cajal at least during 2021–2022, to be active in 2021 and 2022, to not adopt teleworking in 2021 except for the mandatory lockdowns, to not have suffered of any medical sick leave during 2021 because of a physical ailment. The exclusion criteria were: to practice exercise more than 8h per week, to have suffered a condition during 2021 other than mild to moderate respiratory illness, to present vital signs of over- or underweight. All the participants had higher education and received no compensation for their participation in the study. The demographic characteristics of the participants are shown in Table 1.

The procedure consisted of a previously scheduled appointment for each participant (day and time); at that appointment an interview was held to collect the participant information before selection, and for those included in the experiment, to schedule a day and time for the tests. All tests were taken by each participant in a single morning. All the subjects were tested on weekday mornings (from 10 a.m. to 1 p.m.) and the whole process for all the subjects took 1 month.

Table 1. Demographics of subjects participating in the study.

Total Number		21		
Sex	Men	7		
	Women	14		
Age	≤25	4	Men	2
			Women	2
	26 < x < 40	9	Men	3
			Women	6
	>40	8	Men	2
			Women	6
Exercise	Sedentary	14	Men	4
			Women	10
	Exercised	7	Men	4
			Women	3

2.2. Tests

The test battery consisted of five different protocols: virtual path integration, real path integration, virtual hidden goal task, real-space hidden goal task and real-space multiple-choice maze. The order to perform the tests was randomly chosen except for when a virtual and a real-space version of the same test are used. In these cases, the virtual version has to be performed before and followed by the real-space one. We first describe our new circular maze (Technical section, Section 2.3), and second the protocols of the tests (Functional section, Section 2.4).

2.3. Technical Section

Circular maze: we built a cylindrical structure with a conical roof, measured 3 m tall by 3 m in diameter (Figure 1). The structure consists of four columns, just under 3 m, attached on the top to a ring that doubles as support for the roof beams and a curtain rail. The roof is slightly slanted with its higher point in the middle (at 3 m of height). We covered the whole structure with blackout curtains so no light coming from the outside could be used as a spatial cue, a circular piece covers the roof and eight overlapping curtains hang from the rails. Everything in the structure is made of hollow aluminum to simplify cable management, transportation and assembly. On the middle point of the roof, on the inside, there is a small circular plate for attaching electronic components. Holes were drilled in each column facing the center of the structure, so we could attach electronics and pass power cables. Every column has its own electrical outlet which is powered by a single master plug.

For the electronics inside the structure, we use five Raspberry Pis version 4 (one for each of the four columns and one on the roof), four 32 × 32 Adafruit RGB LED Matrices, four Adafruit RGB Matrix HATs, two MG996r servo motors, a KY-008 laser module, a bread board, a Noir Camera V2 module and the respective connection and power wires.

We took four electrical junction boxes and drilled holes on the back and on the lid of each one. Then we glued the matrices to the lids, passed the matrices wires through the lid hole, connected them to the Adafruit HATs inside the box (which were themselves connected to the Raspberry Pis) screw the boxes to their respective columns and powered everything through the hole of the back of the box with the plug that comes out of the hole of each column. Another power wire was also threaded through a roof beam to power the remaining Raspberry Pi, two servos and the laser module.

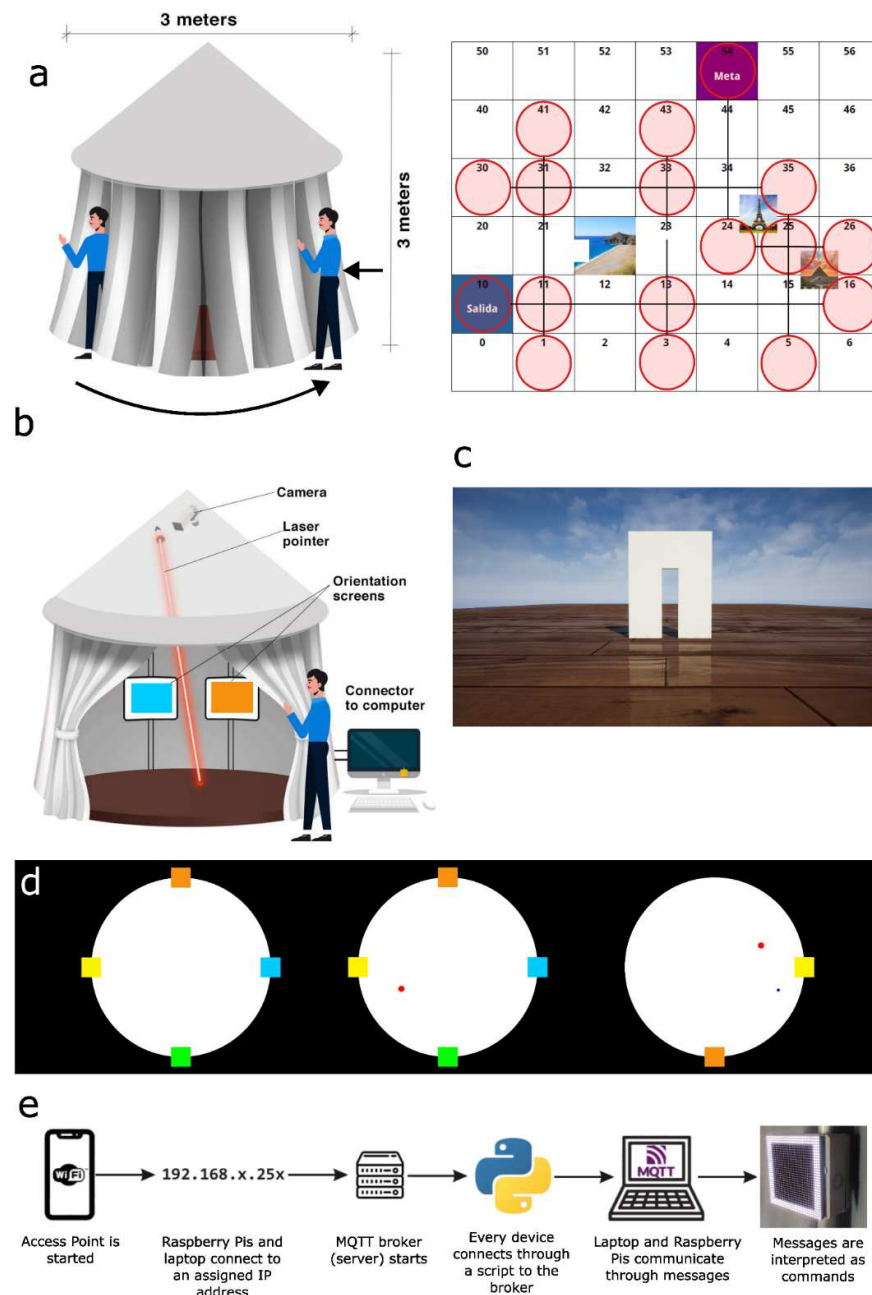


Figure 1. Overview of the spatial navigation tests. (a) Scheme of the maze test in the multi-test circular arena designed and built for this work. Note that the same arena has been used for both real-space hidden goal test and the multiple-choice maze-like task (a,b). To the left, exterior appearance of the tent showing how participants have to enter, exit, and go around. To the right, the map designed to implement the multiple-choice maze-like task. It is represented with North at the upper side of the scheme. Note that several paths can be chosen at some of the points, some cul-de-sacs exist, and the movements chosen do not necessarily lead to a linear displacement. The small pictures represent the few spatial cues that appear in the wall screens when the participant enters at the appropriate locations in the map. For example, the Eiffel tower is visible from locations 24, 25, and 35 on the screen that is at the appropriate direction (northeast, northwest, and southwest, respectively). There is only one circular arena, each time participants exit, they must reenter the arena by the opposite entrance the test ends when participants arrive at position 54. (b) Real-space hidden goal task, the tent is represented with open curtains to see 2 of the 4 screens of the wall and the roof devices. The aim of this test is to remember the laser position on the floor respectively to the position of the cues in the screens. (c) Screenshot of the program built in our lab to implement the virtual path integration

test (made with Unreal). It shows the floor, the sky, and the door through which the participant must pass to move into the next step of the task (a new door at a different position) participants must then return to the starting point of the test. (d) Examples of the appearance of the program built in our lab to implement the virtual hidden goal test. To the left, the circular maze with the spatial cues in the walls. Center, the goal is represented by a red dot. The participant must learn its relative position to the spatial cues. Right, a typical test with only some of the spatial cues shown. The subjects have to point an X–Y position inside the white circle where they think the hidden goal test is located (in this case, a tiny blue point). After a few seconds, the real position of the goal appears on the screen (blue dot). One more test was performed in our study, the real space path integration test (not depicted) where subjects must walk blindfolded through a pre-established path to then return to the beginning of it. (e) Information flow in the circular structure.

This approach greatly simplifies dealing with possible malfunctions or future modifications in two main ways: firstly, the box lid can be opened to access every component inside. Over and above that, due to the ease of assembly, each box can be thought of as a module, allowing us to have several entire boxes ready (containing every electrical device and wires) so we could simply unplug the old one and plug the new one should any malfunction happen.

The whole structure can be disassembled and reassembled in a matter of hours using only regular Philips screwdrivers and a step ladder. It can also be transported in a small van and placed anywhere with access to the electrical grid and cellular coverage.

Although every electrical component is connected to the same electrical network, there is no wired data sent between Raspberry Pis, since we chose to use wireless communication (Figure 2). To achieve this, we created and configured a WiFi access point (via android portable hotspot feature). We then burnt five MicroSD cards with the Raspberry Pi OS image, editing the `wpa_supplicant` configuration file on each SD card, adding the Service Set Identifier (SSID) and password of the previously created network to make a headless setup. The headless setup was conducted through the Secure SHell (ssh) protocol via a laptop on the same network and consisted of updates, upgrades, OS setup and installation of required packages and libraries (such as the Henner Zeller LED-matrix).

After the initial setup, we soldered the pin headers and terminal block to each adafruit HAT and connected them to their respective Raspberry Pis, matrices and 5V DC power. Once every matrix display was checked for errors, we attached the servomotors, laser, camera, breadboard and breadboard power supply to the circular plate on the roof. Both the servos and the laser were connected by the ground wire to the breadboard and by the control wire to the General-Purpose Input Output (GPIO) ports on the Raspberry Pi, the live wire on the servos was also connected to 5V on the breadboard. The camera module was directly connected to the Raspberry Pi through a ribbon cable.

We needed the laser to be able to point at every possible point of the floor beneath the structure. To achieve this, we attached the laser module to the first servo motor, pointing it down at the center of the floor when in its middle position. At this point the laser can only oscillate in a straight line from 90 degrees forward to 90 degrees backwards. To reach 360 degrees, we attached this laser and servo to the second servo, making it so that the axis of rotation of the second one is perpendicular to the first one and their middle positions parallel and in the same direction. Using two perpendicular axes of rotation, the whole floor region of the structure can be thought of as a two-dimensional Cartesian coordinate system. Since we know the height at which the laser was attached to, we could easily translate real-life distances on the floor to servo motor angles using Pythagoras's theorem (which was later automated with a python script). The camera was fixed to the central part of the roof pointing straight down, later programmed to be in synchrony with the laser and servos.

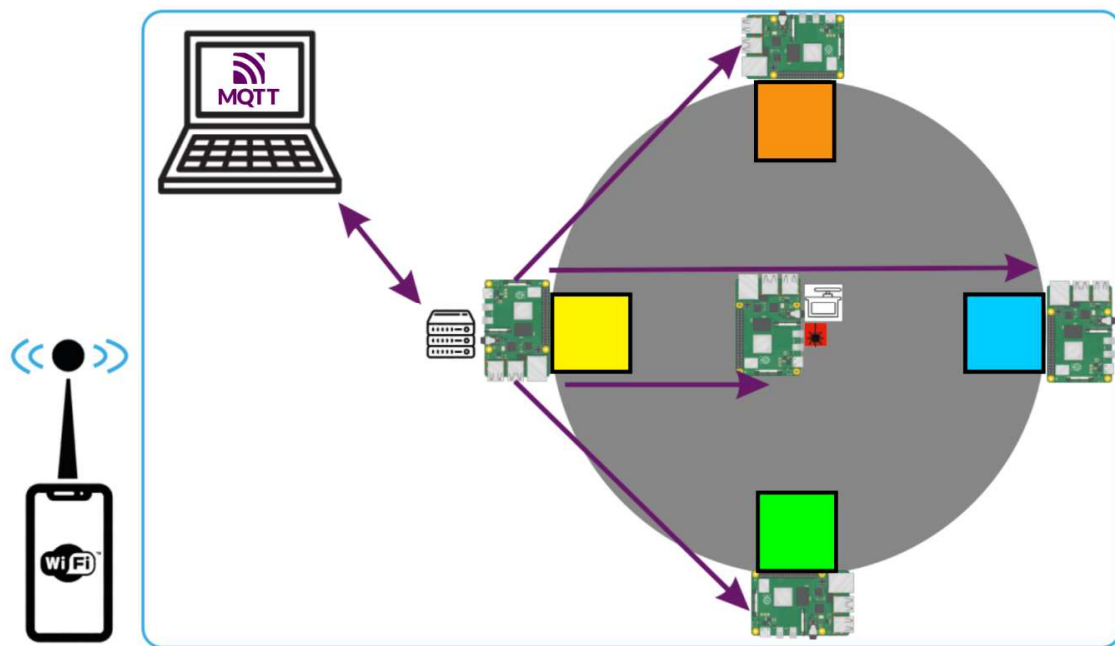


Figure 2. Global architecture and connections scheme. Android device (left) sharing a WiFi access point (represented by the blue square where every device is). Laptop sending and receiving MQTT messages from and to the Raspberry Pi that acts as broker (server icon on the left) placed in a column of the circular structure (grey circle). Every other Raspberry Pi in the columns and ceiling (the center one) reads messages and act accordingly, either changing the output of the screens (represented as colored squares) or shining a laser on the floor or taking pictures in the case of the Raspberry in the roof.

For wireless communication we decided to use the MQTT protocol over the WiFi network that we previously created. We made one of the Raspberry Pis double as both a broker and a client, and the rest of the Raspberry Pis and a laptop were configured only as clients.

The information flow starts on the laptop, which runs several programs that we wrote to publish and read different messages to the broker. These messages are sent through one of seven different MQTT topics, depending on which experiment is running at a time, which phase it is in, which device sends it, and which one is supposed to read it.

Every device is running programs to constantly read the messages sent to certain topics on the broker and check for matches in a closed list of possible messages. When a device (e.g., the Raspberry Pi on the northwestern column) reads a certain message on a specific topic (e.g., message “2a” to topic “allocentric/trials”) it will perform a given action (e.g., display an orange square on the led matrix). Raspberry Pis also send messages to the broker for the laptop to read as a means of reporting to the experimenter what every device inside the structure is doing in real time. This approach allows us to send a single message (that can be associated with a button click on the computer, or automated with a timer) and have six different devices performing a list of different actions upon reading it.

2.4. Functional Section

Virtual path integration: Path integration tests address the internal cues-based spatial. Internal cues are provided by our head direction system, vestibular system (angular head direction and linear acceleration), the proprioceptive system, the optic flow, and the motor efference copy [1]. This navigation implies “an internal tracking of direction and distance” [1]. As all these components depend on the body and head movement, as well as visual record of both the cues and the path, these tests are usually performed by both virtual (visual) and real (non-visual) protocols. For the virtual path integration test, we adapted the largely reported virtual environments by using our own software program. We

programmed a three-dimensional virtual environment using Unreal Engine 4. This environment consisted of a 63 m × 63 m square floor (6300 × 6300 unreal units, 1 u.u. = 1 cm), a skybox and a door frame.

Subjects can freely move around, within the borders of the environment, by pressing W, A, S and D on the keyboard (to walk forward, left, back and right, respectively). The camera is controlled with the movement of the computer mouse. The aforementioned door frame is programmed to detect when a participant walks through it; this event is used as a trigger for changing the position of the frame through the map (three times, once at a time). After subjects are fully briefed on the movement control scheme, the protocol goal is explained to them. They are instructed to walk through the door frame, look for where it has moved to, and repeat until it entirely stops reappearing (it requires four passes). After it disappears, subjects are to return, as close as they are able to, to the starting point of the test and communicate it to the experimenter. The experimenter can then press a key on the keyboard that reports the distance in pixels between where the participant indicated and the real starting point. This distance is used as the participant's score. The positions of the door frames are: first door 7.2 m from start position, right to the front. Second door 35 m 60° to the left, third door 28.5 m 115° to the right, fourth door 28.5 m 130° to the right. From this last position, the participant has to manage to go back to the starting position, 35 m 60° to the right.

After the virtual path integration test is completed, we proceed to its physical counterpart.

Real-space path integration: We accommodated the frequently used protocols for real-space path integration to our facilities. Subjects are taken to a wide-open space with no obstacles, where the experimenter explains the protocol. Once subjects understand the procedure, they have to blindfold themselves on the starting position of the trial (position zero) and then grab with both hands a meter-long rod that the experimenter is holding parallel to the floor at chest height. The experimenter is then to guide the participant to the four different points of the area by dragging the rod as they walk. After the participant arrives at each point, the experimenter stops, informs them of which point it is (e.g., first, second . . .), turns them to the direction of the next point and walks to it in a straight line. This process is repeated until the fourth point is reached. Once at the fourth point, the participant (still blindfolded) has to return to the point zero (in a straight line, not by walking through the four previous points they walked by). The experimenter is still holding the rod without exerting any force on it, only to prevent the participant from colliding with their surroundings. Once the participant arrives at where they think point zero is, they stay in place, take off the blindfold and put one end of a measuring tape between their feet. The experimenter takes the other end and measures the distance to the point zero. This distance is used as the participant's score. The distances and angles between points are as follows: point zero to point one 7.3 m in a straight line. Point one to point two 7.9 m after a 90+ degree right turn. Point two to point three 12 m after a 150 degree turn right. Point three to point four 15.8 m after 150 degrees turn left.

Participant and experimenter now move to the Laboratory of Human Behavior booth where the circular maze is located.

Virtual hidden goal task: Hidden goal tasks are well-known spatial navigation tests used for both rodents and humans, consisting of finding a non-visible target guided only by external spatial cues. The version for humans is usually considered most similar to the water maze test for rats and mice [29]. For both the virtual and the real-space tests, we used an adaptation of protocols published elsewhere [30]. Before starting the virtual allocentric protocol, the experimenter gives the participant a written protocol with images (Supplementary Materials), explaining how the program is controlled and what the goal of the test is. Subjects are told to read the instructions as many times as they need and to ask any question to the experimenter. Once the participant understands the procedure, the experimenter runs the virtual allocentric computer program on the laptop. This program asks the experimenter to input the subject's name (for later storage of results). After that, the protocol begins with the first trial.

Each trial in both the virtual and the physical protocol is structured around a memorization phase followed by four recall phases. This trial is repeated (with different cues to memorize) a total of three times in each protocol (so each participant goes through a total of three memorization phases and twelve recall phases).

The virtual allocentric protocol consists of a computer program that displays a top-down representation of the physical structure, with four cues on the positions where the columns would be (a big white circle representing the floor beneath the structure and cues 90 degrees from each other on the edge of the circle representing the led matrices on the columns, Figure 1d left). Subjects have the time they need to memorize which cue is on each of the four positions (they have been instructed to memorize the relative position, not the absolute position, that is the relation and order of cues between each other and not the individual positions on the computer screen; “cue 2 is between cues 1 and three and opposite to cue 4” instead of “cue 2 is on the northeast”). Once they consider they have memorized the cues relative positions, they communicate it to the computer program by clicking with the mouse left button anywhere on the computer screen. When the program registers the first click, it displays a red dot somewhere on the floor of the virtual structure signaling the position of the goal (Figure 1d center). Both the cues and the goal are displayed simultaneously on the screen for fourteen seconds for the participant to memorize. After these fourteen seconds pass, the memorization phase is over, cues and goal are removed and recall phase one starts.

Recall phases reduce the number of cues displayed (by two on the first, second and third phases and by three on the fourth) and randomly rotate them (around the central point of the virtual structure floor) either 90 or 180 degrees, clockwise or anticlockwise (Figure 1d, right).

On recall phase one, two out of the four cues are displayed, not on their original locations on the screen but randomly rotated (e.g., if cues rotated 90 degrees clockwise the cue that was on the eastern column on memorization phase now is on the southern, the southern on the western, etc.) always maintaining the original distances with each other displayed on the memorization phase. Participant now has to click on the place of the screen where the goal should be. Computer records the distance in pixels from the place participants clicked and the real location of the goal. This distance is used as the participant's score.

Real-space hidden goal task. In the physical protocol the experimenter begins by executing the corresponding software (by running a script on the laptop that automatically sends a command through ssh to every device). The Raspberry Pis on the columns show a white square on the matrices to illuminate the interior of the structure and to signal that the software started running. The Raspberry on the roof will point the laser (without turning it on) straight down from whichever position it was pointing to.

On the laptop, the experimenter is asked to write the subject's name and press the Enter key. When done, two messages are sent from the laptop to the broker in different topics: the first one contains the subject's name (which is sent by a topic that only the Raspberry on the roof is programmed to read) and will be used to name the photographs that the camera takes. The second message is a start signal. When the start signal is read the white square changes to the corresponding images in the first memorization phase, depending on which Raspberry reads it. After 14 s, the laptop sends another message signaling the Raspberry on the roof to move the laser to the precise coordinates the goal should be on, turns the laser on, takes a picture, saves it with the subject's name and the trial number and blinks the laser five times in rapid succession in case the participant has not seen it by then. When the laser turns off, the laptop sends the first message of the recall phase, each Raspberry displaying its corresponding “recall phase, trial 1” image.

In the recall phase the participant has to recognize the cue pattern of the matrices and signal the part of the floor which they think the laser will now shine on. The participant is given a 30-cm diameter wooden disk with a LED in the center top part and a meter-long

handle. The participant is instructed to place the center of the disk in the position they think the laser will appear.

The images on the screen are displayed for 14 s (or until the participant places the disk on the floor). After that, another message is sent to repeat the laser-camera routine (simultaneously changing the cues and laser absolute placement but maintaining their relative positions). This recall-laser procedure repeats a total of four times after each memorization phase. There are three different memorization phases, each one with a different queue configuration and goal placement.

After the last trial, every picture the Raspberry Pi saved with the subject's name is sent to the laptop via Secure CoPy (SCP) protocol. Using ImageJ [31] we can measure the distance in pixels from the laser to the LED on the wooden disk the participant placed. The sum of the error in every trial is the final score in this protocol.

Real-space multiple-choice maze. This test was entirely designed in our laboratory to measure the spatial navigation abilities of human beings in a complex maze, in real space, but all enclosed in a reduced space. The main objective is to compare the results obtained from this test to those from the rest of the tests. The participants have to orientate guided by intra-maze spatial cues to find a path from the starting to the target point following a map. The same arena (the circular maze) is used now, but this time the participants exit the maze when necessary and re-enter by another position. This procedure is repeated many times to recapitulate a complex maze until the target is reached. The same laptop, hardware, and screens are used, but in this protocol a different program is executed on the laptop; since this protocol requires multiple (but standardized) inputs from the experimenter, a Graphical User Interface (GUI) was added using pygame. Several buttons, an input box and output terminal were included in the program.

Like in the previous protocol, the experimenter has to execute the appropriate programs on each device. Again, this step is performed by running a script on the laptop that sends commands through ssh to each device. Once every device is running the egocentric protocol program, the experimenter can execute the GUI on the laptop. On the GUI, when the experimenter clicks the "Start Trial" button, a timer starts, and a message is published on the broker to initialize the led matrices with the first position of the maze.

In this protocol participants take one of four possible routing decisions (north, south, east and west) and the matrices have to react accordingly to that decision. The way we approached this is by hanging signs outside the structure indicating cardinal points. Subjects have to exit the structure, inform the experimenter of what cardinal point they chose and come back to the structure through the opposite cardinal point (see why below). The experimenter will then click one of the corresponding buttons on the program. This will publish a message to the broker, the Raspberry Pis on the columns will read it and change the image on the matrices accordingly to the new position the participant will arrive at. Subjects also have to inform the experimenter of which square they think they are at each movement.

Subjects are asked to exit the structure in the general direction that they want to move through the maze. Once outside the structure, they are instructed to walk around it and go back inside through the opposite entrance (e.g., walk out the north exit and reenter through the south). The reason is to preserve the movement component in this task, since we wanted participants to navigate through real space. If the participants exit and reenter through the same exit, this would not preserve the orientation of the maze and the navigation as a whole; if the maze was real and subjects exited a room through the eastern exit, they would arrive at the westernmost entrance of the next room.

To evaluate the real-space multiple-choice maze-like test, we considered first to use a holistic score that would represent the subjects' performance. However, this test has different dimensions not strictly related, and summarizing them in a single value would cause a loss of information. The variables we registered were: the positions visited by the subject, the movements (directions), their predictions of the present position at each time, time spent between movements. Other variables can be inferred from these, such

as how many times a specific position was visited, whether the participant tried to do an invalid movement, the total time spent into the maze, where they were at a specific time, the distance to the goal, the relative speed, etc. None of these variables on their own is descriptive enough to inform about the performance of a participant in the whole test. Total time does not describe how many positions the participant visited, how accurate their predictions were, or if their movements took them closer or further to the goal.

To address this problem, we considered two independent measurements: prediction error and decision (movement) error. Total prediction error is the sum of every prediction error through the entire test. Prediction errors are measured as Manhattan distance and not as Euclidean distance. Manhattan distance is the number of movements that it would take to get from the position the participant thinks they are to the real position they are. So, if the participant predicts they are two movements away from where they really are, the prediction error would be two (in that particular prediction). A low total prediction error shows that the participant was right and aware of their position during the test.

Total decision error is a measurement that reflects how effective the subjects' movements are through the test. To calculate it we gave an arbitrary penalty to each possible movement in the map (0.2 for good movements and 1 for bad movements). We considered good movements as every movement towards the general direction of the goal when possible. If the four cardinal points are possible movements, and the goal is in the northeast, both north and east movement decisions would be given a 0.2 penalty while south and west would both be given a 1. This penalty is then multiplied by the number of times that the participant has already been in the movements' resulting position. The first time a bad movement take the participant to a certain position the penalty is 1, but the third time (if it occurs) would be 3, and so on. A lower total decision error reflects better choice of movements, 1.4 being the minimum possible error (because the goal is at least seven movements away from the start, and whether every movement that take the participant to the goal is considered good; 0.2 penalty).

2.5. Factor and Level Analysis

We have taken into consideration several variables to categorize the subjects and to analyze the results: participant variables (sex, age, total number of hours of exercise per week), hidden goal test variables (distance error, either in cm for real-space or in pixels for virtual, total time in virtual), path integration variables (distance error, either in cm for real-space PI, or in pixels for virtual), multiple-choice maze-like variables (direction error, prediction error, total time to exit from the maze), ratio variables (path integration, virtual score/real space score; hidden goal test, virtual score/real space score).

As for the levels, age was categorized when necessary in three groups: <25 years old; 26–40 years old; >40 years old. Total time of exercise in two groups: sedentary (<3 h/week) or exercise (>3 h/week). Maze performance: low or high errors (for both prediction and direction errors).

2.6. Statistical Analysis

Extreme values were removed from the analysis of the specific variable for which it was extreme. Other non-extreme outliers were not removed from the analysis. Outliers were detected using R's package *Rstatix*, with the function "*identify outliers*". This function evaluates where every value fall within the distribution of a specific variable. This package criterion to define an outlier is to be above $Q3 + 1.5 \times IQR$ or below $Q1 - 1.5 \times IQR$. $Q3$ being quartile 3, and IQR being InterQuartile Range ($Q3 - Q1$). As such, a value is considered extreme while above $Q3 + 3 \times IQR$ or below $Q1 - 3 \times IQR$. Extreme values were taken off both analysis and figures, non-extreme outliers were preserved in both.

Normality tests were conducted for all the variables by Shapiro–Wilk test. In the correlation analysis, Pearson's correlation coefficient was used in all cases, as it does not assume normality in the variables. A value of $R \geq |0.4|$ was used as threshold for plotting correlations (moderate correlations or stronger, criteria by Evans 1996 [32]).

Mean comparisons. Normal variables (total time in labyrinth) were analyzed by one-way ANOVA. Non-normal variables (the rest of variables) were analyzed as follows:

- Kruskal–Wallis for non-parametric variables with more than two grouping levels.
- Wilcoxon for pair comparisons of the significant results from the Kruskal–Wallis (adjusting the p by the Benjamini–Hochberg method) and for non-parametric variables with less than two grouping levels.

The comparison between virtual and real space tests was made by dividing virtual by real space scores (virtual/real ratio) for each subject. The individual ratio was then grouped as described (see above) and analyzed to detect differences by Kruskal–Wallis. When significant, the comparison was analyzed by Wilcoxon for pair comparisons adjusting the p .

In all cases, the level of significance is $p < 0.05$. Statistics were done using R Version 4.2.0, graphics used the packages ggplot2 (v3.3.6), ggpubr (v0.4.0), and dlokr (v0.6.0) and inkscape (Inkscape Project).

3. Results

We have developed a system to evaluate the spatial navigation abilities of freely-moving humans in real space. It consists of a circular maze containing electronic devices connected to a computer, plus a dedicated protocol to test spatial navigation, simulating a complex maze into a small enclosure. The circular maze is similar to a tent, with four vertical openings in a blackout curtain (Figure 1a left). Inside the enclosure, four electronic screens show spatial cues. A laser pointer attached to two electric motors and a video camera are also installed at the center of the roof (Figure 1a right).

We have considered the tent as a modular location in which the participant can enter, orientate, decide where to go, and go out by the appropriate exit, in such a way that the next time they enter the tent, the scenario has changed to that of the next position on the map. This way, the system simulates as if the participant was entering in a new location (see map, Figure 1b). As it can be seen on the map, multiple choices are possible at several locations, so subjects have to evaluate both their position each time, and the direction of their next movement. The cues into the tent will change accordingly to the new location, so the participant will have to orientate again, decide where to go, and exit. With this design, the participant can be evaluated in a complex maze, as big and complex as the experimenter decides it to be, as a function of the age of the subject, experimental design, or scientific question posed.

We have compared this protocol design with validated tests previously reported, both implemented in this same multipurpose system and others implemented in a different arena. To this aim we have also tested the same group of subjects in both a virtual (Figure 1c, see Materials and Methods) and a real-space path integration test, plus a virtual (Figure 1d, see Materials and Methods) and a real-space hidden goal task.

We have tested a group of participants with a wide range of ages (see demographics in Table 1, and Figure 3a), and self-reporting a wide range of mean physical activity per week (Figure 3b). All subjects performed the five orientation tests. In the multiple-choice maze-like spatial navigation task, we found an expected high variability both in the prediction error (Figure 3c) and in the decision error (Figure 3d), and consequently also in the total time spent in the maze (Figure 3e). This variability was also observed in the other four tests, either physical or virtual versions of the path integration test (Figure 3f,g, respectively), and physical (Figure 3h) or virtual hidden goal task (both measuring error (Figure 3i) and time spent in the task (Figure 3j)).

Next, to know the potential either intra- or inter-tests relationships (each measuring different aspects of the general human spatial navigation process) we elaborated a correlation matrix taking into account a number of key measurements of the different tests used here. Pearson's correlation coefficient was used to analyze extensively potential correlations. The main findings can be seen (Figure 4) as a direct (positive) relationship between age and several errors both in virtual and in real space (the older the age, the higher the error in both path integration, and hidden goal test), and the performance in validated tests

such as the hidden goal test or the path integration each other, and both correlated to our new test. Some other significant correlations point to an internal validation of our new test, for example between total time spent in the maze with either the prediction or the decision errors. The matrix also shows a number of interesting non-significant correlations, for example no correlation was found between the performance of virtual vs. real-space path integration (while a correlation does exist between virtual vs. real-space hidden goal task). In the same line, prediction error and decision error in the multiple-choice task did not correlate.

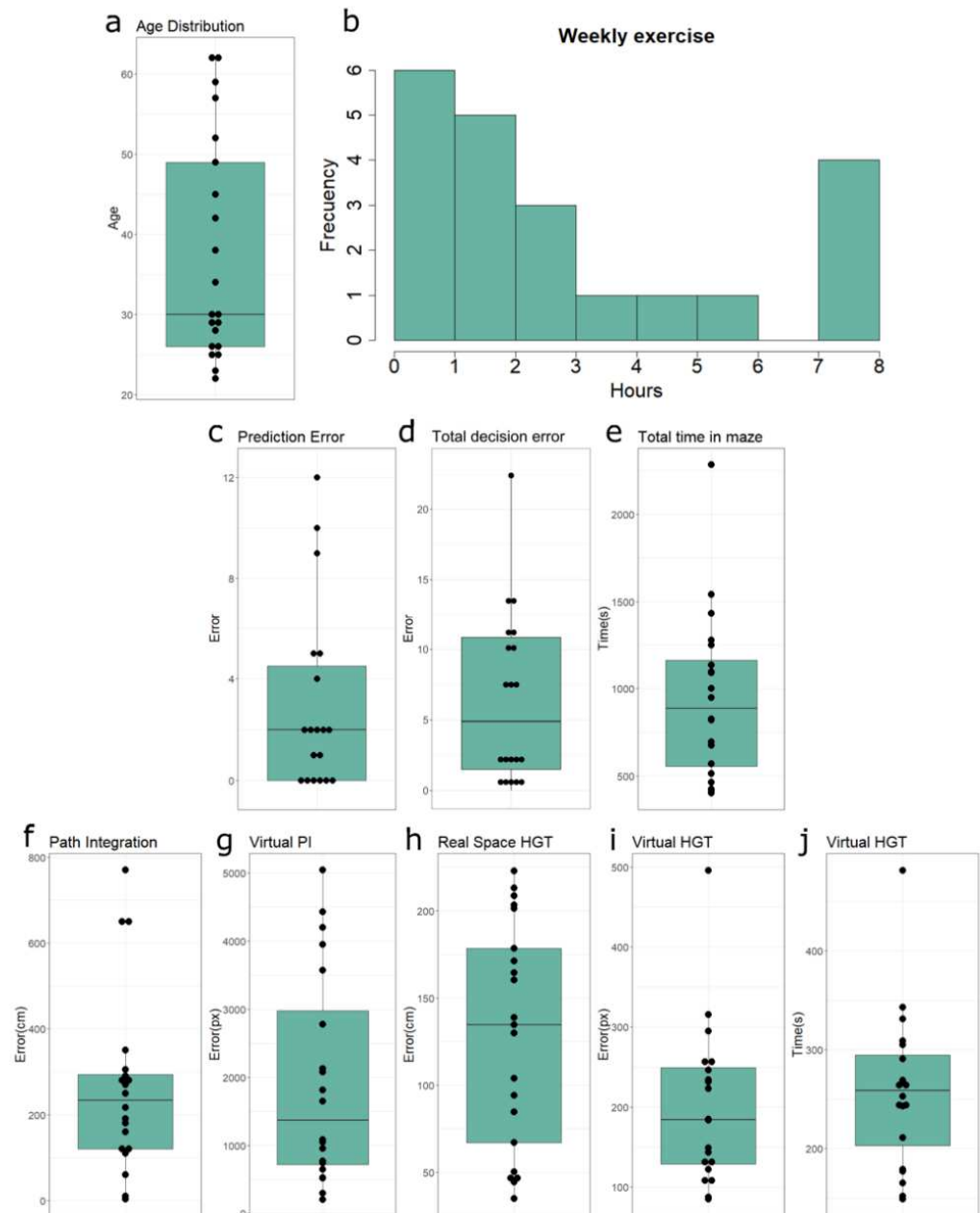


Figure 3. Group distribution and performance in the different tests. The group of participants had a wide age range (a) and was heterogeneous in the number of hours of exercise per week (b). Parameters measured for the multiple-choice maze-like test (c–e), path integration (f,g), and hidden goal test (h–j). A great variability can be seen for all the tests, either real-space (c–f,h) or virtual (g,i,j). Each dot represents 1 person. (PI: Path Integration, HGT: Hidden Goal Task).

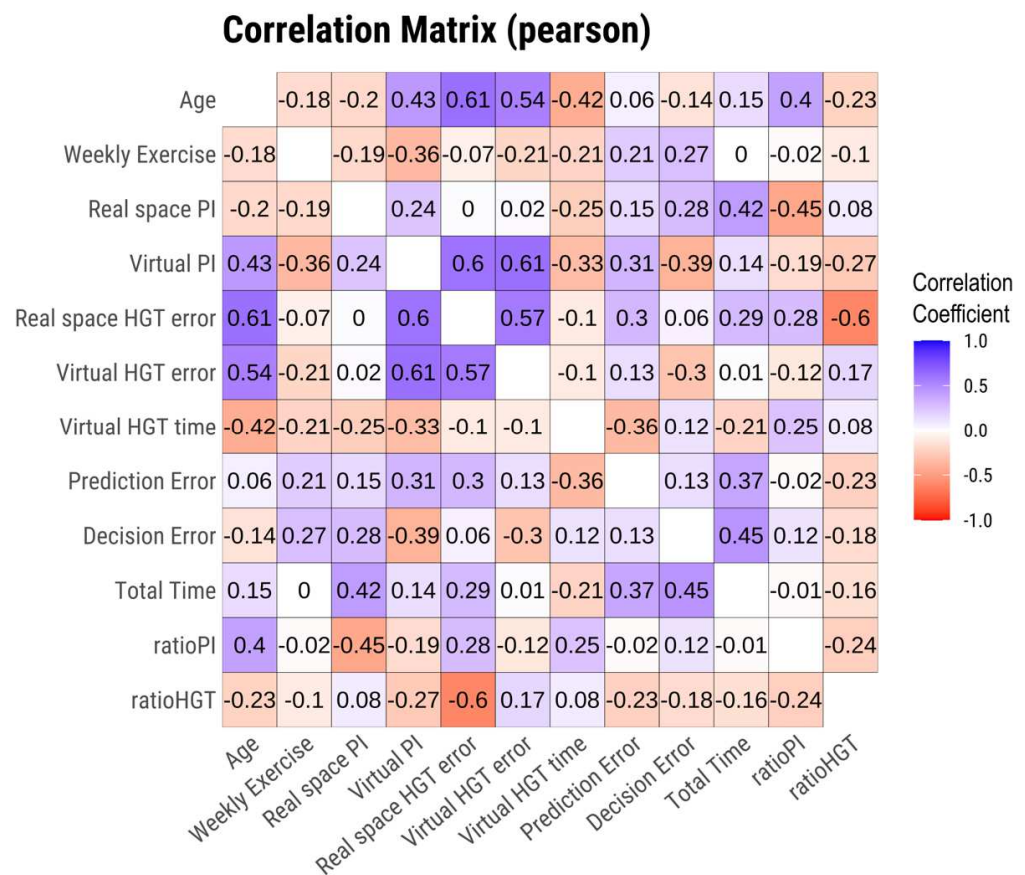


Figure 4. Correlation matrix of key measurements of the different tests. Both positive and negative potential correlations can be seen. Note the higher correlation coefficient between age and performance of some of the tests, and the coefficient between the real-space and virtual versions of the tests. This matrix was used to analyze specific correlations in more detail (Figure 5).

We further analyzed these variables’ relationships in more detail by considering either the new hardware device alone or, independently, the dedicated protocol designed here. We first analyzed the subjects’ performance in a version of a previously validated test into our new maze. We found the subjects’ error in both the real space and virtual versions of the hidden goal test positively correlated each other (Figure 5a, $R = 0.57$, $p = 0.0087$), as expected, being higher with age (Figure 5b,c, $R = 0.61$, $p = 0.032$, $R = 0.54$, $p = 0.013$ respectively), as expected. Consistently, both versions of the hidden goal test significantly positively correlated to the error in the path integration test (Figure 5d,e). Therefore, it is not surprising that although the time spent in the virtual version of the hidden goal test showed a negative correlation (trend, $R = -0.42$, $p = 0.065$) to age, (Figure 5f), the error positively (trend) correlates with age (Figure 5g). The new protocol presented here could be validated in this line consistently, showing a significant positive correlation between decision error and total time into the maze (an internal validation of the task, Figure 5h) and a trend between the total time spent into the maze and the error in the path integration test (validation compared to other tests, Figure 5i). For brevity, only moderate or greater correlations are shown in Figure 5.

There also exists a tendency on the performance on the real-space hidden goal test error on subjects over 25 but under 40 years old where exercised outperform sedentary, which is inverted in subjects over 40 (Figure S1a, $p = 0.06$, $p = 0.57$). By dividing by sex and age, there is no difference in men, but women present a significant difference in age range (<40 years old with higher error, $p = 0.0082$). This difference is still present while subdividing first by age and then by sex: there is no difference in any age range by sex but in the <40 range where there is a tendency (Figure S1c, $p = 0.07$). Regarding the virtual

hidden goal test, there is a tendency in sedentary depending on the age, <40 sedentary people underperform younger sedentary (Figure S1d, $p = 0.077$).

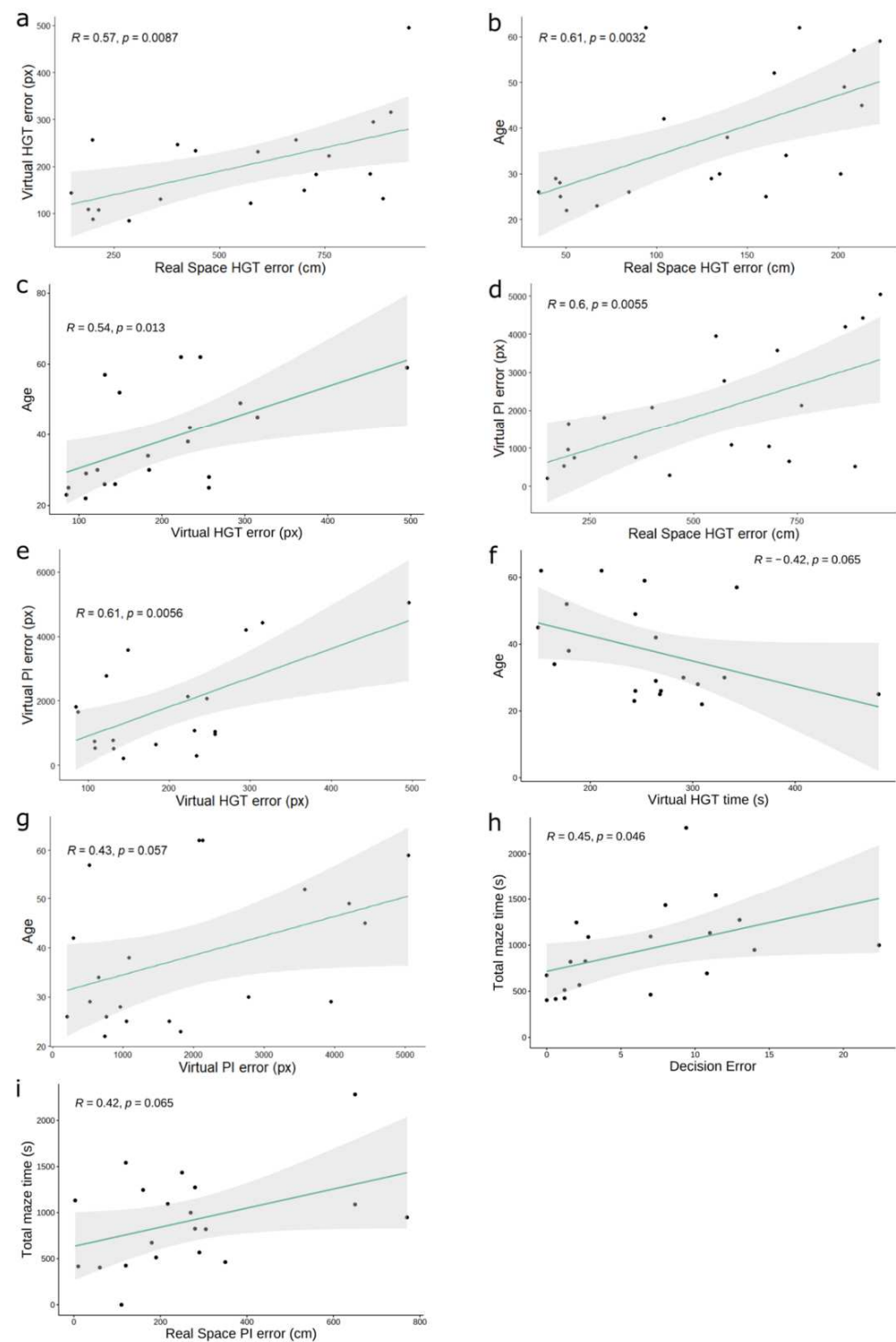


Figure 5. Significance of the main correlations between measurements. (a–h) Correlations of validated tests with each other or with subjects’ age. Significant positive correlations (a–e) can be seen, as well as a trend in the performance of virtual versions of hidden goal test and path integration with age (f,g). A significant correlation was found between the decision error of our new multiple-choice real-space maze and the time spent in the maze (internal validation, h), and a trend between the time spent in the maze with the error in the path integration test (inter-test validation, i). Each dot represents 1 person.

We next proceeded to further examine complex interactions between variables. We found that the error in a real-space hidden goal test increased significantly with age, being higher for subjects older than 40 years old compared to younger subjects (Figure 6a, $p = 0.025$), as expected. Doing so, we found that this error was consistently higher in 40-year-old subjects independently of their weekly physical activity level (Figure 6b, $p = 0.029$). The same relationship between hidden goal test error and age was also found for the virtual version of the task (Figure 6c, $p = 0.04$), as expected.

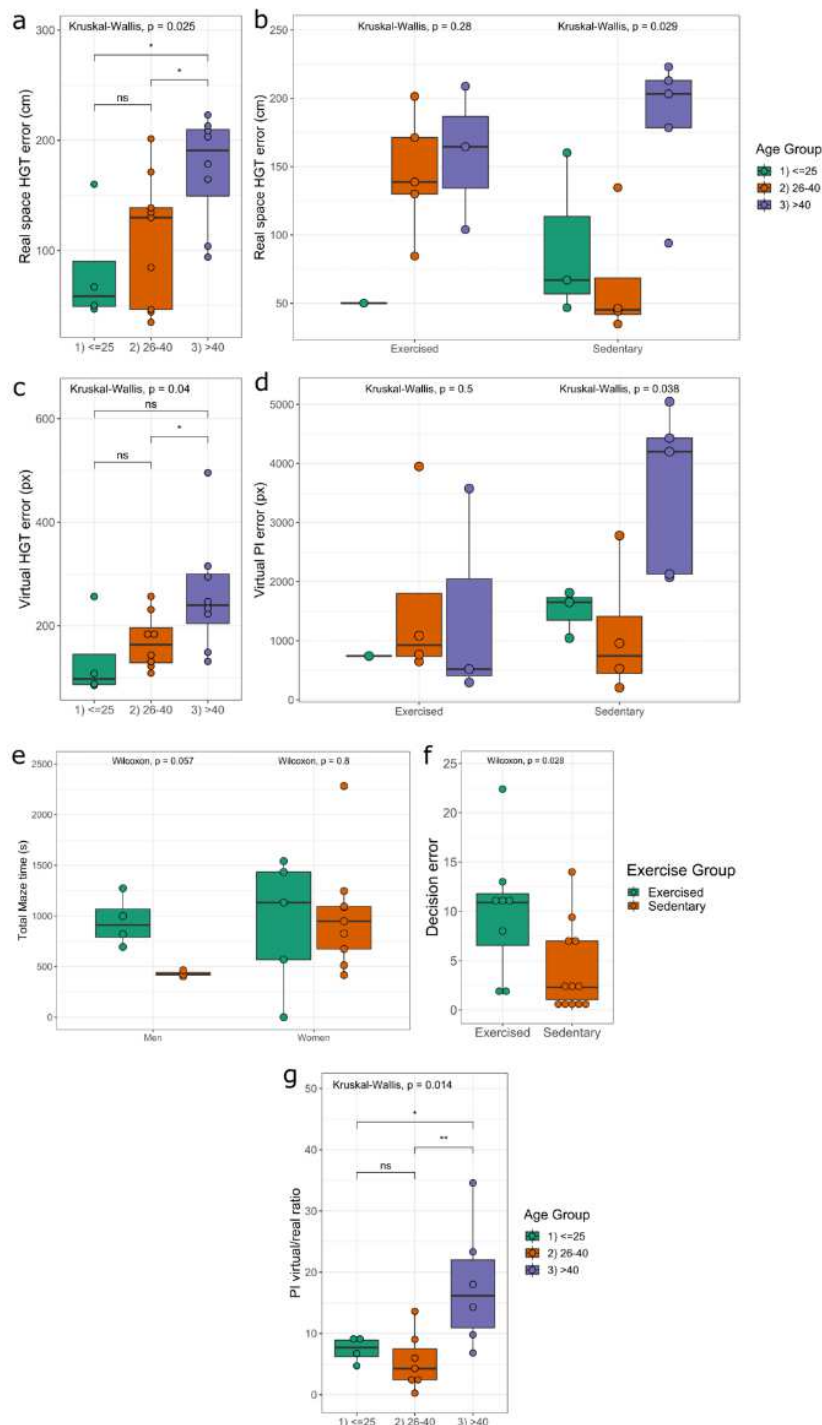


Figure 6. Complex interactions between variables. The relationship between some of the significant results found here depending on several variables was analyzed. Significant differences found between groups (a,c,f,g) and between subgroups (b,d,e) within our study variables. The interaction

between the subjects' age (a–d) and their performance on validated tests (hidden goal and path integration) depends on the subjects' physical activity level, both in real-space (a,b), and virtual versions (c,d). In our new multiple-choice maze-like test (e,f), differences between sex (e) or physical activity level (f) were explored. Differences between virtual versus real-space tests depending on subjects' age were also found (g). * = $p < 0.05$, ** = $p < 0.01$. Each dot represents 1 person. PI: Path integration, HGT: Hidden Goal Task. Effect sizes: a Kruskal-Wallis $\text{Eta}^2 = 0.299$, magnitude: large. a Wilcoxon age groups 1–3 effect size = 0.686, magnitude: large, Wilcoxon age groups 2–3 effect size = 0.537, magnitude: large. b Kruskal-Wallis $\text{Eta}^2 = 0.567$, magnitude: large. (b) Wilcoxon sedentary age groups 2–3 effect size = 0.735, magnitude: large. c Kruskal-Wallis $\text{Eta}^2 = 0.246$, magnitude: large, Wilcoxon age groups 2–3 effect size = 0.499, magnitude: moderate. (d) Kruskal-Wallis $\text{Eta}^2 = 0.505$, magnitude: large, Wilcoxon sedentary age groups 1–3 effect size = 0.791, magnitude: large. € Wilcoxon effect size in men = 0.802, magnitude: large. (f) Wilcoxon effect size = 0.501, magnitude: large. (g) Kruskal-Wallis $\text{Eta}^2 = 0.362$, magnitude: large, Wilcoxon age groups 1–3 effect size = 0.674, magnitude: large, age group 2–3 effect size = 0.713, magnitude: large.

Interestingly, our system was able to detect also a difference between the error in the performance of the virtual version of the path integration test and subjects' age depending on the level of activity (Figure 5d, $p = 0.038$), as expected. Although some other interesting relationships between exercised and sedentary groups might be suggested, the number of subjects precluded any categorical conclusion in this regard (see also Supplementary Figure S1).

These relationships contribute to validating the hardware/device system itself, therefore we next analyzed the ability of the dedicated protocol to detect complex relationships. We found that the total time spent into the maze was similar between men and women (Figure 6e), but a difference between exercised and sedentary subjects was detected (Figure 6f, $p = 0.028$), pointing to the capacity of this new system to detect subtle differences between subjects. The system allowed us to detect also a difference between these subjects' performance in virtual versus real space tests depending on the age (higher score in real space compared to virtual tests for those subjects older than 40 years old, Figure 6g, $p = 0.014$).

4. Discussion

We have compared the evaluation of human spatial navigation obtained with previously validated tests to a new system composed of a multi-test circular arena and a novel protocol simulating a complex maze. Our arena is freely inspired by previously reported circular mazes [28–30] including a new system with a laser beam to point a spot in any position on the floor, inside wall-screens to present spatial cues, and a video camera to track the path and distances, able to recreate many different spatial navigation tests for humans, and versatile enough to implement new protocols. The new system was created with the goal of including free body movement, in a complex maze, in real space, but all enclosed in a reduced space, while allowing evaluation of both egocentric and allocentric navigation, neural activity recording, and difficulty level customization, in all cases if/when required. The dynamic of this new test was created trying to recapitulate the continuous orientation and reorientation one has to perform while navigating spaces where some spatial cues (necessary to find a path) are only available as long as the participant is doing short displacements, such as for example into a department store, where one has to reorientate after going around many repetitive aisle displays (with a similar average size than our system) while advancing from the starting position to a distant target end [33].

The system presents several advantageous features. First, it allows the evaluation of freely moving subjects. This is very relevant for spatial navigation, as the proprioceptive component of movement has long been underrated, especially in the on-screen orientation tests implemented with computers. Recently, head-mounted VR systems or omnidirectional treadmills (reviewed by [1]) have improved the analysis of spatial navigation including vestibular, proprioceptive, and somatosensory cues, although the limitation of the move-

ment still remains a challenge. One solution would be to evaluate the subjects in a large complex maze, but laboratories cannot usually afford it due to the size necessary to implement such an arena. In our system, we have tried to solve this problem by implementing a design including hardware, software, and a dedicated protocol, all allowing to evaluate spatial navigation in freely moving subjects that have to orientate through a complex maze with dead ends and occasional non-linear movements. A usual test to perform our maze takes a mean of 20 min, and the participant walks a mean of 70–80 m during the test, although the circular arena is only 3 m in diameter. This is because the system is designed to recreate a set of different spatial cues on the screens on the inside walls of the arena. This is done in such a way that when the subjects orientate themselves according to the map and the cues, and exit the arena, they have to enter again the arena at a specific different entrance point, and meanwhile the inside scenario has automatically changed through a computer to recreate the new location the participant has chosen to go. This way, the participant can be tested in a complex maze as the experiment requires (see map in Figure 1b) but still in a controlled, reduced space.

This design is useful to customize the difficulty of the test, because the experimenter can easily change the number of locations the participant will have to go to reach the target, the difficulty of the path to transit to those locations, the number of dead-ends and non-linear movements, and the on-screen spatial cues. This is useful to design specific experiments devoted to analyzing spatial navigation with children, adults, elders, neurodegenerative patients, or any other conditions. It allows to measure horizontal properties of several spatial navigation tests such as pattern separation or completion, by modifying the spatial cues. The experimenter could even change some of the system features on the test, depending on the path the participant is following, which can be tracked live in situ. For the same reasons, the system is entirely fit to run experiments with a device measuring live neural activity. As the maze is a discrete, controlled arena, and the environment is enclosed and controlled, it is very easy to use helmets or devices for transcranial magnetic/electric stimulation for the participants. Additionally, sensitivity and quality of human brain activity recording have considerably improved recently in freely moving subjects, by using controlled environments (see for example [34]). These novel preparations can easily be used in our new system to provide correlated measures of neural activity while the subject is actively navigating.

Second, the system is multipurpose to implement many other spatial navigation tests previously reported, such as path integration or hidden goal tests. Third, it is portable, and finally, it allows longitudinal studies by only changing the spatial cues and the path to the goal, e.g., changing the map.

Additionally, being a physical test in real space confers an intrinsic advantage over VR systems to evaluate spatial navigation, which might induce dizziness (mainly to elder people) especially when using VR glasses [35,36]. Besides that, distinct usage rates between the young and elders might reflect disparity in the familiarity in the use of devices [37] rendering it unreliable when comparing different age groups in a study. Last but not least, elder people might have higher disaffection with a new virtual challenge than young people, compared to a new physical challenge, where both age groups may be comparable [38,39].

In our validation study, we have seen that our system yields consistent results with what is expected in known spatial navigation tests such as hidden goal test or path integration. Our measurements of the maze test give us information about three different dimensions: how accurately are participants predicting their own position, how effective is their path-finding, and the total amount of time they take to arrive at the goal. Several difficulties arise when validating this test. Firstly, to our knowledge, there is no other human spatial navigation test consisting of a complex real-space maze measuring subjects' performance. Secondly, these mentioned dimensions are composed of several processes (not purely a path integration task, nor a hidden goal task). And lastly, two of these dimensions (prediction and decision error) are, to a certain degree, independent from each other, while total time may influence both errors (more time in the maze can result in more

movements, and more movements may give rise to more errors). With all this in mind, validation of this test must come from how our results fit within both the literature and the predictions we made based on it.

First, decision error and prediction error do not correlate ($Rho = 0.13$), as expected. Second, both errors show a low to moderate correlation with total time ($Rho = 0.37$ for prediction error and $Rho = 0.45$ for decision error) showing a clear influence, but not a strong correlation. Third, low to no correlation with tests measuring different variables. Fourth, organizing scores by quartiles we can divide our sample by a good/bad performance in each error. Since they are different dimensions, there are participants in every resultant subdivision (low prediction error with low decision error, high prediction error with low decision error, etc.). As expected, making good predictions of their position does not mean good path-finding (61.5% good path-finding), people with bad path-finding indistinctly make good or bad predictions (50%) but people with bad predictions rarely have a low path-finding error (20%). So, while these dimensions are different and do not correlate, knowing one-self's position increase the chance of making good path-finding decisions.

Furthermore, we found a trend of a positive correlation between the time spent to solve the maze and the error in the real-space path integration test. This finding should be expected if a proprioceptive component of spatial navigation is involved in real-space spatial navigation in humans [1] and reinforces the utility of this real-space spatial navigation test to include components of orientation usually not considered [40–42]. The system was able to detect subtle differences in performance depending on age, or on the effect of exercise, especially for specific age groups. This is relevant as it allows to design experiments to test spatial navigation in different contexts as lifestyle, drug interventions, or conditions involving cognition or neurodegeneration.

While all the spatial navigation tests in our new system have so far been egocentric, our system can also be used additionally to easily implement allocentric tests, for example through testing orientation of the subjects into our arena with no spatial cues, only based on a cognitive map the subjects have been previously trained to remember (data in preparation). Therefore, most of these results point to the new system as a valid approach to measure the components of human spatial navigation (because both the significant and the non-significant results provide the expected information following the consensus principles of human navigation [1]) by using a multi-purpose, multiple-choice, complex arena, and a protocol all implemented in a reduced space. The system is able to measure spatial navigation in an environment avoiding some of the main disadvantages of the known tests in the field (e.g., our system includes free body movement in a real space, complex environment, built in a reduced space). Nevertheless, a Limitations section and a Future Directions section are included next to bring out potential concerns to be addressed in the future.

In summary, our system allows the evaluation of human spatial navigation with several distinct types of known tests as well as a new test based on a multiple-choice maze-like task with customizable complexity, all implemented in a small, portable circular arena. It is sensitive enough to detect subtle differences in spatial navigation between age groups or between sedentary vs. exercised subjects, and its results correlated as expected with previously validated orientation tests.

4.1. Limitations

Our system presents potential limitations. When the participants exit the tent to reenter at a different entrance, they have to perform a short semicircular displacement into the booth, out around the tent. To avoid distractions in this short displacement, we asked the participants to concentrate in the map and their next movement. The participants reported at the end of the test that they were not aware of the environment while performing the test. Additionally, the mentioned strategy directly contributes to removing any vestibular component of the navigation process, thereby depending heavily on the cognitive map.

The performance score method was entirely designed de novo as this is a new test with multiple choices, precluding to use simple variables. For example, the time spent to find the target is not a good parameter to evaluate the spatial navigation ability in this system, as it depends entirely on what paths the participants chose when more than one choice was available and equally good (see methods). Therefore, although this scoring system is artificial and based on compound variables, the ex profeso design was made to exclude of the formulae any non-spatial navigation component.

Consistently, the time is not a crucial factor in this system, although this may lead to a long test duration for some subjects. As this may be a problem causing very different time duration for different participants, we restricted the total number of tests per session to five.

The presence of both virtual and real-space versions of some tests makes it advisable to run first the virtual version and then the real-space one. This ensures that the performance of the test was not entirely random. The influence of the order to perform the tests in the results must be further tested in the future.

Finally, although this study would benefit from a larger sample size (in the exercised <25-years-old subgroup there is only one participant), since our results already fit within the theoretical frame depicted in the literature, and results fall under our initial predictions, we do believe the test is validated.

4.2. Future Directions

This system can be used immediately to measure both degenerative impairments in spatial navigation and the potential improvement of any intervention or therapy designed to address spatial navigation. However, a necessary first step is to test as many different participants subgroups in this system as possible, for example, children/teens, adults, and elderly people. In the same line, both healthy and stressed subjects, as well as the effects of lifestyle will for sure provide very interesting information about human spatial navigation.

Nevertheless, joint evaluation of neural activity correlated with performance of spatial navigation is a promising subfield to generate relevant information about the dynamics of navigation. Furthermore, this information can be easily contrasted with individual molecular profiles of selected, hypothesis-driven lists of potential mediators of different interventions (as for example epigenetic effectors). All this information might be used, in turn, to design personalized therapies or lifestyle interventions that would be tested with this system.

Supplementary Materials: The following supporting information can be downloaded at: <https://www.mdpi.com/article/10.3390/app12199707/s1>, Figure S1: Other complex interactions between variables.

Author Contributions: Conceptualization, P.M., E.C., P.T., A.O., L.L.-M. and J.L.T.; Formal analysis, P.M., E.C., P.T., R.G.B. and J.L.T.; Investigation, P.M.; Methodology, P.M., E.C., P.T., B.F.-G., C.T.-Z., E.I.-G., A.E.D.M., R.G.B., V.C.-P., R.D.I.V., V.S.-L., A.O., L.L.-M. and J.L.T.; Resources, P.M., B.F.-G., C.T.-Z., E.I.-G., A.E.D.M., V.C.-P., R.D.I.V., V.S.-L., A.O., L.L.-M. and J.L.T.; Software, P.M.; Supervision, J.L.T.; Validation, P.M. and J.L.T.; Visualization, P.M., E.C. and P.T.; Writing—original draft, J.L.T.; Writing—review & editing, P.M. and J.L.T. All authors will be informed about each step of manuscript processing including submission, revision, revision reminder, etc. via emails from our system or assigned Assistant Editor. All authors have read and agreed to the published version of the manuscript.

Funding: P.M. was funded by a predoctoral fellowship (FPI) grant, PRE2020/093032, from the Ministerio de Ciencia e Innovación; E.C. was funded by a predoctoral fellowship (FPI) grant, BES-2017/080415, from the Ministerio de Economía y Competitividad; P.T. was funded by a predoctoral fellowship (FPU) grant, 18/00069, from the Ministerio de Universidades. This research received no other external specific funding.

Institutional Review Board Statement: The study was conducted according to the guidelines of the Declaration of Helsinki, and approved by the CSIC Ethics Committee (Subcommittee of Ethics) of the Spanish Research Council, ref. no. 036/2021, 04/19/2021.

Informed Consent Statement: Informed consent was obtained from all subjects involved in the study.

Data Availability Statement: All materials, data and associated protocols used in this work are available to interested readers.

Acknowledgments: All the work, supplies, and expenses have been kindly provided from the scientists and participants participating in the study. We are grateful to José Manuel Cañizares for building the structure, to the Director of the Institute Cajal for his support to the project and managing the outside booth housing the maze, to Raúl Muñoz from the Infrastructure Department of Institute Cajal for the setup and building the booth, to Juan C. Moreno from the Neural Rehabilitation Group of the Institute Cajal for his support to the project facilitating the access to the high performance computer, to Marta Montero and Inmaculada Molina from the Institute Cajal, for their help with the research, to A2Colores staff for the graphics of the maze, and to all the participants participating in the study.

Conflicts of Interest: The authors have no conflict of interests to declare.

References

- Ekstrom, A.D.; Spiers, H.J.; Bohbot, V.D.; Rosenbaum, R.S. *Human Spatial Navigation*; Princeton University Press: Princeton, NJ, USA, 2018; ISBN 978-0-691-17174-6.
- Tuena, C.; Mancuso, V.; Stramba-Badiale, C.; Pedroli, E.; Stramba-Badiale, M.; Riva, G.; Repetto, C. Egocentric and Allocentric Spatial Memory in Mild Cognitive Impairment with Real-World and Virtual Navigation Tasks: A Systematic Review. *J. Alzheimers Dis. JAD* **2021**, *79*, 95–116. [[CrossRef](#)] [[PubMed](#)]
- Montello, D.R. Navigation. In *The Cambridge Handbook of Visuospatial Thinking*; Miyake, A., Shah, P., Eds.; Cambridge Handbooks in Psychology; Cambridge University Press: Cambridge, UK, 2005; pp. 257–294. ISBN 978-0-521-80710-4.
- Patai, E.Z.; Spiers, H.J. The Versatile Wayfinder: Prefrontal Contributions to Spatial Navigation. *Trends Cogn. Sci.* **2021**, *25*, 520–533. [[CrossRef](#)] [[PubMed](#)]
- Banquet, J.-P.; Gaussier, P.; Cuperlier, N.; Hok, V.; Save, E.; Poucet, B.; Quoy, M.; Wiener, S.I. Time as the Fourth Dimension in the Hippocampus. *Prog. Neurobiol.* **2021**, *199*, 101920. [[CrossRef](#)] [[PubMed](#)]
- Mobbs, D.; Wise, T.; Suthana, N.; Guzmán, N.; Kriegeskorte, N.; Leibo, J.Z. Promises and Challenges of Human Computational Ethology. *Neuron* **2021**, *109*, 2224–2238. [[CrossRef](#)]
- Moffat, S.D.; Kennedy, K.M.; Rodrigue, K.M.; Raz, N. Extrahippocampal Contributions to Age Differences in Human Spatial Navigation. *Cereb. Cortex* **2007**, *17*, 1274–1282. [[CrossRef](#)]
- Kim, B.; Lee, S.; Lee, J. Gender Differences in Spatial Navigation. *World Acad. Sci. Eng. Technol.* **2007**, *31*, 297–300.
- Munion, A.K.; Stefanucci, J.K.; Rovira, E.; Squire, P.; Hendricks, M. Gender Differences in Spatial Navigation: Characterizing Wayfinding Behaviors. *Psychon. Bull. Rev.* **2019**, *26*, 1933–1940. [[CrossRef](#)]
- Zanco, M.; Plácido, J.; Marinho, V.; Ferreira, J.V.; de Oliveira, F.; Monteiro-Junior, R.; Barca, M.; Engedal, K.; Laks, J.; Deslandes, A. Spatial Navigation in the Elderly with Alzheimer’s Disease: A Cross-Sectional Study. *J. Alzheimers Dis. JAD* **2018**, *66*, 1683–1694. [[CrossRef](#)]
- Yu, S.; Boone, A.P.; He, C.; Davis, R.C.; Hegarty, M.; Chrastil, E.R.; Jacobs, E.G. Age-Related Changes in Spatial Navigation Are Evident by Midlife and Differ by Sex. *Psychol. Sci.* **2021**, *32*, 692–704. [[CrossRef](#)]
- Turgeon, M.; Lustig, C.; Meck, W.H. Cognitive Aging and Time Perception: Roles of Bayesian Optimization and Degeneracy. *Front. Aging Neurosci.* **2016**, *8*, 102. [[CrossRef](#)]
- Plácido, J.; de Almeida, C.A.B.; Ferreira, J.V.; de Oliveira Silva, F.; Monteiro-Junior, R.S.; Tangen, G.G.; Laks, J.; Deslandes, A.C. Spatial Navigation in Older Adults with Mild Cognitive Impairment and Dementia: A Systematic Review and Meta-Analysis. *Exp. Gerontol.* **2022**, *165*, 111852. [[CrossRef](#)] [[PubMed](#)]
- Cammisuli, D.M.; Cipriani, G.; Castelnuovo, G. Technological Solutions for Diagnosis, Management and Treatment of Alzheimer’s Disease-Related Symptoms: A Structured Review of the Recent Scientific Literature. *Int. J. Environ. Res. Public Health* **2022**, *19*, 3122. [[CrossRef](#)] [[PubMed](#)]
- Lithfous, S.; Dufour, A.; Després, O. Spatial Navigation in Normal Aging and the Prodromal Stage of Alzheimer’s Disease: Insights from Imaging and Behavioral Studies. *Ageing Res. Rev.* **2013**, *12*, 201–213. [[CrossRef](#)] [[PubMed](#)]
- Gazova, I.; Vlcek, K.; Laczó, J.; Nedelska, Z.; Hyncicova, E.; Mokrisova, I.; Sheardova, K.; Hort, J. Spatial Navigation—a Unique Window into Physiological and Pathological Aging. *Front. Aging Neurosci.* **2012**, *4*, 16. [[CrossRef](#)] [[PubMed](#)]
- Parizkova, M.; Lerch, O.; Moffat, S.D.; Andel, R.; Mazancova, A.F.; Nedelska, Z.; Vyhnalek, M.; Hort, J.; Laczó, J. The Effect of Alzheimer’s Disease on Spatial Navigation Strategies. *Neurobiol. Aging* **2018**, *64*, 107–115. [[CrossRef](#)]
- Stuchlik, A.; Kubik, S.; Vlcek, K.; Vales, K. Spatial Navigation: Implications for Animal Models, Drug Development and Human Studies. *Physiol. Res.* **2014**, *63*, S237–S249. [[CrossRef](#)]
- Fellous, J.-M.; Dominey, P.; Weitzenfeld, A. Complex Spatial Navigation in Animals, Computational Models and Neuro-Inspired Robots. *Biol. Cybern.* **2020**, *114*, 137–138. [[CrossRef](#)]

20. Issa, J.B.; Tocker, G.; Hasselmo, M.E.; Heys, J.G.; Dombek, D.A. Navigating Through Time: A Spatial Navigation Perspective on How the Brain May Encode Time. *Annu. Rev. Neurosci.* **2020**, *43*, 73–93. [[CrossRef](#)]
21. Wei, E.X.; Anson, E.R.; Resnick, S.M.; Agrawal, Y. Psychometric Tests and Spatial Navigation: Data From the Baltimore Longitudinal Study of Aging. *Front. Neurol.* **2020**, *11*, 484. [[CrossRef](#)]
22. Laczó, J.; Vlcek, K.; Vyhnálek, M.; Vajnerová, O.; Ort, M.; Holmerová, I.; Tolar, M.; Andel, R.; Bojar, M.; Hort, J. Spatial Navigation Testing Discriminates Two Types of Amnesic Mild Cognitive Impairment. *Behav. Brain Res.* **2009**, *202*, 252–259. [[CrossRef](#)]
23. Laczó, J.; Andel, R.; Vyhnálek, M.; Vlcek, K.; Magerova, H.; Varjassyova, A.; Tolar, M.; Hort, J. Human Analogue of the Morris Water Maze for Testing Subjects at Risk of Alzheimer's Disease. *Neurodegener. Dis.* **2010**, *7*, 148–152. [[CrossRef](#)] [[PubMed](#)]
24. Laczó, J.; Andel, R.; Vyhnálek, M.; Vlcek, K.; Magerova, H.; Varjassyova, A.; Nedelska, Z.; Gazova, I.; Bojar, M.; Sheardova, K.; et al. From Morris Water Maze to Computer Tests in the Prediction of Alzheimer's Disease. *Neurodegener. Dis.* **2012**, *10*, 153–157. [[CrossRef](#)] [[PubMed](#)]
25. Schöberl, F.; Zwergal, A.; Brandt, T. Testing Navigation in Real Space: Contributions to Understanding the Physiology and Pathology of Human Navigation Control. *Front. Neural Circuits* **2020**, *14*, 6. [[CrossRef](#)] [[PubMed](#)]
26. Diersch, N.; Wolbers, T. The Potential of Virtual Reality for Spatial Navigation Research across the Adult Lifespan. *J. Exp. Biol.* **2019**, *222*, jeb187252. [[CrossRef](#)] [[PubMed](#)]
27. Park, J.L.; Dudchenko, P.A.; Donaldson, D.I. Navigation in Real-World Environments: New Opportunities Afforded by Advances in Mobile Brain Imaging. *Front. Hum. Neurosci.* **2018**, *12*, 361. [[CrossRef](#)] [[PubMed](#)]
28. Bažadona, D.; Fabek, I.; Babić Leko, M.; Bobić Rasonja, M.; Kalinić, D.; Bilić, E.; Raguž, J.D.; Mimica, N.; Borovečki, F.; Hof, P.R.; et al. A Non-Invasive Hidden-Goal Test for Spatial Orientation Deficit Detection in Subjects with Suspected Mild Cognitive Impairment. *J. Neurosci. Methods* **2020**, *332*, 108547. [[CrossRef](#)] [[PubMed](#)]
29. Kalová, E.; Vlcek, K.; Jarolímová, E.; Bures, J. Allothetic Orientation and Sequential Ordering of Places Is Impaired in Early Stages of Alzheimer's Disease: Corresponding Results in Real Space Tests and Computer Tests. *Behav. Brain Res.* **2005**, *159*, 175–186. [[CrossRef](#)]
30. Laczó, J.; Markova, H.; Lobellova, V.; Gazova, I.; Parizkova, M.; Cerman, J.; Nekovarova, T.; Vales, K.; Klovrzova, S.; Harrison, J.; et al. Scopolamine Disrupts Place Navigation in Rats and Humans: A Translational Validation of the Hidden Goal Task in the Morris Water Maze and a Real Maze for Humans. *Psychopharmacology* **2017**, *234*, 535–547. [[CrossRef](#)]
31. Schindelin, J.; Arganda-Carreras, I.; Frise, E.; Kaynig, V.; Longair, M.; Pietzsch, T.; Preibisch, S.; Rueden, C.; Saalfeld, S.; Schmid, B.; et al. Fiji: An Open-Source Platform for Biological-Image Analysis. *Nat. Methods* **2012**, *9*, 676–682. [[CrossRef](#)]
32. Evans, J.D. *Straightforward Statistics for the Behavioral Sciences*; Thomson Brooks/Cole Publishing Co: Belmont, CA, USA, 1996; ISBN 0-534-23100-4.
33. Grewe, P.; Lahr, D.; Kohsik, A.; Dyck, E.; Markowitsch, H.J.; Bien, C.G.; Botsch, M.; Piefke, M. Real-Life Memory and Spatial Navigation in Patients with Focal Epilepsy: Ecological Validity of a Virtual Reality Supermarket Task. *Epilepsy Behav.* **2014**, *31*, 57–66. [[CrossRef](#)]
34. Topalovic, U.; Aghajan, Z.M.; Villaroman, D.; Hiller, S.; Christov-Moore, L.; Wishard, T.J.; Stangl, M.; Hasulak, N.R.; Inman, C.S.; Fields, T.A.; et al. Wireless Programmable Recording and Stimulation of Deep Brain Activity in Freely Moving Humans. *Neuron* **2020**, *108*, 322–334.e9. [[CrossRef](#)] [[PubMed](#)]
35. Lin, C.-H.; Lin, H.-C.; Chen, C.-Y.; Lih, C.-C. Variations in Intraocular Pressure and Visual Parameters before and after Using Mobile Virtual Reality Glasses and Their Effects on the Eyes. *Sci. Rep.* **2022**, *12*, 3176. [[CrossRef](#)] [[PubMed](#)]
36. Lubetzky, A.V.; Kelly, J.; Wang, Z.; Gospodarek, M.; Fu, G.; Sutura, J.; Hujsak, B.D. Contextual Sensory Integration Training via Head Mounted Display for Individuals with Vestibular Disorders: A Feasibility Study. *Disabil. Rehabil. Assist. Technol.* **2022**, *17*, 74–84. [[CrossRef](#)] [[PubMed](#)]
37. Olson, K.E.; O'Brien, M.A.; Rogers, W.A.; Charness, N. Diffusion of Technology: Frequency of Use for Younger and Older Adults. *Ageing Int.* **2011**, *36*, 123–145. [[CrossRef](#)] [[PubMed](#)]
38. Richardson, C.; Bucks, R.S.; Hogan, A.M. Effects of Aging on Habituation to Novelty: An ERP Study. *Int. J. Psychophysiol. Off. J. Int. Organ. Psychophysiol.* **2011**, *79*, 97–105. [[CrossRef](#)]
39. Behforuzi, H.; Feng, N.C.; Billig, A.R.; Ryan, E.; Tusch, E.S.; Holcomb, P.J.; Mohammed, A.H.; Daffner, K.R. Markers of Novelty Processing in Older Adults Are Stable and Reliable. *Front. Aging Neurosci.* **2019**, *11*, 165. [[CrossRef](#)]
40. Wang, J.; Pan, Y. Eye Proprioception May Provide Real Time Eye Position Information. *Neurol. Sci. Off. J. Ital. Neurol. Soc. Ital. Soc. Clin. Neurophysiol.* **2013**, *34*, 281–286. [[CrossRef](#)]
41. Renault, A.G.; Auvray, M.; Parseihian, G.; Miall, R.C.; Cole, J.; Sarlegna, F.R. Does Proprioception Influence Human Spatial Cognition? A Study on Individuals With Massive Deafferentation. *Front. Psychol.* **2018**, *9*, 1322. [[CrossRef](#)]
42. Nguyen, D.; Truong, D.; Nguyen, D.; Hoai, M.; Pham, C. Self-Controlling Photonic-on-Chip Networks with Deep Reinforcement Learning. *Sci. Rep.* **2021**, *11*, 23151. [[CrossRef](#)]